JOURNAL OF SOLID STATE CHEMISTRY 106, 48–54 (1993)

Valence Loss Electron Spectroscopy of Ni–Al Mixed Oxides

F. J. CADETE SANTOS AIRES, A. HOWIE, AND C. A. WALSH

Cavendish Laboratory, Madingley Road, Cambridge CB3 0HE, United Kingdom

Received December 4, 1992; accepted December 23, 1992

IN HONOR OF SIR JOHN MEURIG THOMAS ON HIS 60TH BIRTHDAY

An outline is given of the extension of the classical theory of dielectric excitation to deal with the spatially localized valence electron spectroscopy of inhomogeneous media. The valence spectroscopy technique has been applied to mixed oxides of Ni and Al. The results have then been interpreted in terms of this extended theory. Significant variations in the position of the main collective loss peak were noted at different points on the samples and are tentatively ascribed to the presence of internal voids or pores rather than to variations in composition. Valence loss spectroscopy may thus provide a means of assessing local pore volume in mixed oxide catalysts. © 1993 Academic Press, Inc.

Introduction

Some of the achievements of electron spectroscopy carried out in the context of an electron microscope were described some years ago in a valuable survey by J. M. Thomas and his colleagues (*1*). Potentially the technique is a very powerful adjunct to high resolution, structural imaging, although the day may only just be approaching when it becomes possible to carry out both procedures in the same instrument without serious compromises. Two significant developments which have taken place in the intervening years have been first the widespread adoption of truly effective instrumentation for parallel recording of the energy loss intensity distribution and second the substantial improvement in the theory for interpreting the valence loss part of the spectrum. As part of the latter aspect, our focus here is on the classical theory of dielectric excitation and its extension beyond the confines of homogeneous media. The ability to deal with the local variations in structure and composition so characteristic of the many materials of practical importance which demand the attention of the electron microscopist is opening up new frontiers for spatially resolved, valence loss spectroscopy. Mixed oxide systems are an excellent example which illustrates the operation of this extended theory and the potential it offers for the improved characterization of complex microstructures.

Dielectric Excitation Theory for Inhomogeneous Media

Because of its high intensity relative to the core excitation part of the electron energy loss spectrum, the valence excitation region has always seemed attractive to electron microscopists. More than twenty years ago, pioneering results in microanalysis as well as physics were obtained (for references, see (*2*)), mainly on free electron alloys, using the sensitivity to valence electron density shown by the position of the prominent (plasmon) loss peak. The energy loss spectra from local regions were recorded by incorporating in the column of

0022-4596/93 $5.00

a transmission electron microscope suitable energy-dispersive electron-optical elements, such as a Mollenstedt cylindrical lens or a Castaing–Henry system. When the advent of scanning transmission electron microscopy (STEM) combined with efficient magnet sector spectrometers opened up the whole spectrum for practical use, attention was redirected to the higher loss, core excitation region since the interpretation of the results there is relatively straightforward. In the last few years, however, the classical dielectric theory, originally developed by Fermi (*3*) for valence excitation by a point charge moving in a homogeneous medium, has been extended and quantitatively checked in a number of situations of interest in electron microscopy. As a result, there has been renewed interest in exploiting some of the advantages of localized valence electron spectroscopy.

Fermi showed that in a homogeneous medium the probability of energy loss $\Delta E = \hbar\omega$ by a nonrelativistic moving charged particle is described by the bulk loss function

$$F_B(\omega) = \mathrm{Im}\{-1/\varepsilon(\omega)\} = \varepsilon_2/\{(\varepsilon_1)^2 + (\varepsilon_2)^2)\}, \quad (1)$$

where $\varepsilon(\omega) = \varepsilon_1(\omega) + i\varepsilon_2(\omega)$ is the complex, frequency-dependent dielectric function. The bulk loss function can evidently exhibit peaks coinciding with maxima in $\varepsilon_2(\omega)$ and arising from single electron excitations from either valence or core levels just as in optical or X-ray absorption processes. In addition, however, peaks in the bulk loss function can arise from the minima in the denominator of Eq. (1), e.g., when $\varepsilon_1(\omega) = 0$ and $\varepsilon_2(\omega)$ is small. The most prominent peak in the valence region of the loss spectrum from many materials turns out to be of this latter type and is associated with a collective excitation of the whole valence system rather than a single electron excitation. The widespread occurrence of these collective losses can be illustrated by reference to the simplest expression for the dielectric function of an insulator with a band gap $E_g = \hbar\omega_g$.

$$\varepsilon(\omega) = 1 - \frac{(ne^2/\varepsilon_0 m)}{\omega(\omega + i\gamma) - \omega_g^2}. \quad (2)$$

where n is the valence electron density and γ is a small damping constant. A collective loss or plasmon will arise at an energy loss $\Delta E = \hbar\omega_p$ where $\varepsilon = 0$ and thus for $\omega_p^2 = (ne^2/\varepsilon_0 m) + \omega_g^2$. This example reduces to the case of a free electron metal referred to above if we take $\omega_g = 0$. In many insulators, however, where the collective excitation energy greatly exceeds the band gap (e.g., in diamond where $\hbar\omega_p = 32$ eV and $\hbar\omega_g = 6$ eV), the collective excitation can be quite similar to a free electron plasmon and be strongly influenced by the valence electron density.

In the early microanalysis work (*2*), it was assumed that the relation between ω_p and n established for a homogeneous medium, could also be applied at the local level in an inhomogeneous situation. While this must be valid for slowly varying situations, it has been recognized more recently that quite new excitations can arise in regions where the dielectric properties vary rapidly with distance. Ritchie (*4*) first identified the surface plasmon excited at a free surface which is a special example for the application of a loss function F_p characteristic of a planar interface between two media A and B.

$$F_p = \mathrm{Im}\{-2/(\varepsilon_A + \varepsilon_B)\}. \quad (3)$$

For a planar interface between a medium A and vacuum we find from this expression the relation $\omega_s^2 = (ne^2/2\varepsilon_0 m) + \omega_g^2$ for the surface plasmon frequency ω_s if we take $\varepsilon_B = 1$ and use Eq. (2) for ε_A. Spherical interfaces are another case of obvious practical importance. Fujimoto and Komaki (*5*) observed the dipole surface excitation of a small sphere of material A embedded in another material B and described by the characteristic loss function F_s

$$F_s = \mathrm{Im}\{-3/(\varepsilon_A + 2\varepsilon_B)\}. \quad (4)$$

The action of these different loss functions has now been quantitatively tested near a variety of isolated interfaces as a

function of impact parameter in STEM (for references, see (*6*)). In general we find a linear combination of various loss functions. As the interface is approached, the amplitude of the interface loss function increases and there is a corresponding drop (*begrenzungseffekt*) in the bulk loss function. In some cases the results at the interface are well described by the simple interface functions given above, but in other cases where some anomalous interfacial layer is present, a more complex loss function corresponding to an appropriate sandwich structure has to be used (*6, 7*). These cases provide some evidence that the detailed analysis of valence loss spectra near interfaces can sometimes yield high resolution information about interface structure or composition not accessible by other methods.

The theory of planar interfaces has also been extended (*8*) to include relativistic effects such as Cerenkov radiation losses which are important when the electron velocity exceeds $c/\sqrt{\varepsilon_1(\omega)}$ (the velocity of light in the medium). Cylindrical interfaces (*9*) and spherical interfaces in higher multipole excitations have also been studied for trajectories both external (*10, 11*) and internal (*12*) to the sphere. Interactions between two spheres have also been analyzed (*13*) but further work is needed for the case of a sphere near a planar interface since previously published solutions (*14*) for this geometry do not appear to be correct (*15*).

In many cases the sample of interest may contain regions so densely packed with defects that individual interfaces or other features cannot be resolved because of overlap effects. These regions may, however, exhibit interpretable effects in the valence loss spectrum. Examples include colloidal dispersions of small clusters (*16*), dealuminated zeolites (*17*) heterogeneous catalysts with highly porous supports containing metal clusters and highly structured materials for absorption of solar radiation. The concept of an effective medium theory to model the dielectric behavior of these materials goes back to Maxwell though many more recent theories have been developed, mainly to deal with optical absorption data or conductivity data. In attempting to apply these existing theories to explain energy loss spectra from such samples, it has been found (*16*) that a somewhat simpler intuitive model often gives considerably better results. In this approach, the effective loss function is modeled as a linear combination of characteristic loss functions of the kind just described. Thus for small clusters of a material A dispersed in a material B one would use an effective loss function given by the expression

$$F_{\text{eff}} = \text{Im}\{-1/\varepsilon_{\text{eff}}(\omega)\} = X\,\text{Im}\{-1/\varepsilon_A(\omega)\} + Y\,\text{Im}\{-1/\varepsilon_B(\omega)\} + Z\,\text{Im}\{-3/(\varepsilon_A(\omega) + 2\varepsilon_B(\omega))\}, \quad (5)$$

where the coefficients X, Y, Z are determined by the particle size and volume fraction and $X + Y + Z = 1$. This approach has even been applied (*18*) with moderate success to model the way in which the loss function of a zeolite depends on pore volume as a result of the increasing interface contribution.

Energy Loss Spectroscopy of Mixed Oxide Samples

The Ni–Al mixed oxide samples were produced by coprecipitation methods similar to those described in detail by Sohier *et al.* (*19*), and were provided by the University of Lille as part of a joint EEC collaboration. Specimens for electron microscopy were then produced by standard methods of crushing under methanol, ultrasonic dispersion followed by deposition on to holey or lacey carbon films supported on copper or aluminum grids. Samples of relevant pure oxides were also examined to yield dielectric data for calibration purposes.

From an experimental loss spectrum in a homogeneous material, the bulk loss function $F_B = \text{Im}(-1/\varepsilon(\omega))$ can be derived following some standard procedures (*20*) to correct for aperture effects and multiple

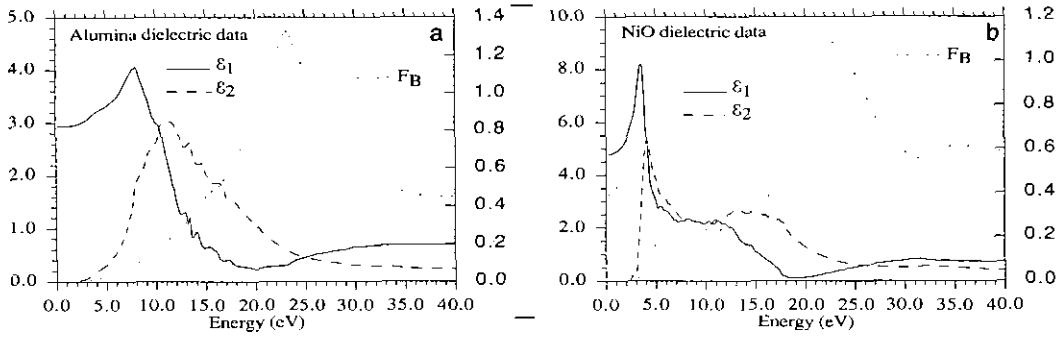

FIG. 1. Dielectric functions (a) for alumina (*21*) and (b) for NiO (supplied by Yuan Jun). In each case ε_1 and ε_2 are plotted on the left-hand scale and bulk loss functions F_B on the right.

scattering. A Kramers–Kronig transformation then yields $\mathrm{Re}(-1/\varepsilon(\omega))$ and hence $\varepsilon_1(\omega)$ and $\varepsilon_2(\omega)$. Figs. 1a and 1b show the bulk loss function F_B, together with the real and imaginary parts of the dielectric function determined in this way for Al_2O_3 (*21*) and NiO respectively. The major peak in both loss functions at 23 eV is clearly of collective (plasmon) type, since it lies just above a near zero of ε_1 rather than at a maximum of ε_2. The rise in ε_2 from zero, which can be seen at low energies, occurs at the band edge but may not be entirely accurate in this region since relativistic corrections have not been applied.

In the mixed oxide samples, small (<10 nm diameter) particles of NiO could be discerned mixed with similarly sized particles of amorphous alumina. Fig. 2a shows spectra obtained from a larger 15 nm NiO particle at the edge of a hole, with the beam first passing through the particle (I), then exactly at the edge of the particle (i) and finally at a distance of about 1 nm into the vacuum outside the particle (v). In Fig. 2b we show for comparison the results of some computations made for these three situations. Clearly the theory successfully provides a qualitative description of the shift of the spectra to lower energies on moving to the

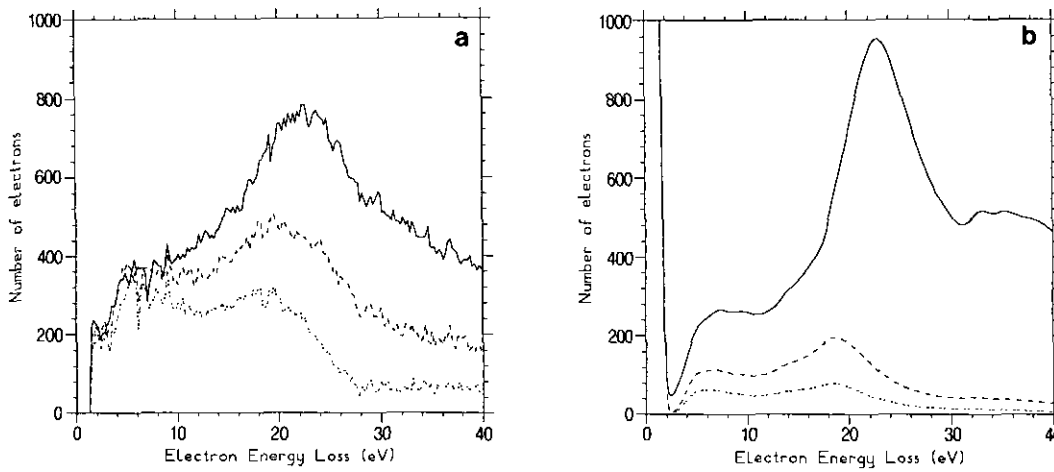

FIG. 2. Loss spectra obtained (—) at the center (I), (– –) at the edge, and (- -) 1 nm outside (v) of a 15-nm diameter isolated NiO particle. Experimental data are shown in (a), computations in (b).

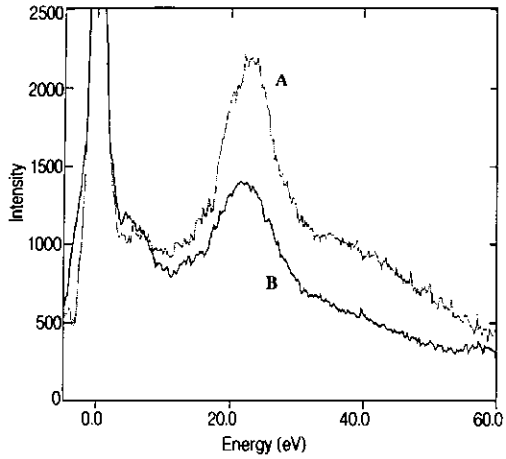

FIG. 3. Loss spectra taken from two different regions A and B of an alumina–NiO mixed oxide showing the variable position of the plasmon loss peak.

outside of the particle but seriously overestimates the drop in intensity.

Studies of interior regions of the mixed oxide gave loss spectra broadly consistent with the bulk loss functions shown in Fig. 1 but quickly revealed significant variations in the position of the main valence loss peak from one point on the sample to another. An example is shown in Fig. 3. In addition to the major change in intensity of the peak, which may be partly due to local changes in effective thickness, the two regions A and B give an energy shift of almost 2 eV. This large shift cannot arise from any local variation in chemical composition since the core loss spectra in the two regions are rather similar as shown in Fig. 4. In any case a local change in the $NiO–Al_2O_3$ ratio would not be expected to show much effect since both oxides give a bulk loss at 23 eV. In principle a shift might result from the formation of a new mixed oxide compound but we did not observe any other evidence of one. Our studies of one such possible compound namely $NiAl_2O_4$ revealed moreover a bulk loss peak at 23.5 eV. A downward shift could perhaps occur if there had been substantial local reduction of NiO to Ni since the latter exhibits a plasmon loss at 21.3 eV. The Ni $L_{2,3}$ edges shown in Figure 4a both display, however, the white lines characteristic of the oxide (*22*).

The many internal interfaces evidently present in the mixed oxide samples could perhaps provide an explanation for some shift in the plasmon peak position. In Fig. 5 the characteristic loss functions for various planar interfaces are shown. Since the dielectric functions of NiO and alumina are rather similar in the relevant energy region, it is perhaps not too surprising that the NiO–alumina interface shows a peak at the unshifted position of 23 eV. However, the planar interface between either oxide and vacuum shows a surface excitation at a substantially lower energy of 20 eV. A population of small voids might be a more appropriate microstructural basis for a dielectric model rather than planar interfaces and the characteristic loss functions for this case (shown in Fig. 6 and derived from Eq. (4) with $\varepsilon_A = 1$) both show a peak at 21 eV. While such a downward shift from the bulk loss position at 23 eV might go some way to explaining the experimental results, a very large volume fraction of voids would clearly be required in some parts of the thin sample if the observations were to be modeled using Eq. (5) with contributions from only the bulk loss function and from the void loss function. A much bigger downward shift of the loss peak is shown by the loss function for a small isolated spherical particle of either NiO or alumina as is shown in Fig. 7. Only a relatively small contribution of this type would therefore be required. In reality of course the sample consists of a rather dense aggregate of particles which will interact dielectrically, so a much more elaborate model may ultimately be necessary.

Conclusions

Spatially localized valence loss spectroscopy would seem to offer considerable potential in conjunction with other electron microscopical techniques in addressing the problem of characterizing the fine-scale microstructure of mixed oxides. Even in an unfavorable case, such as NiO–alumina

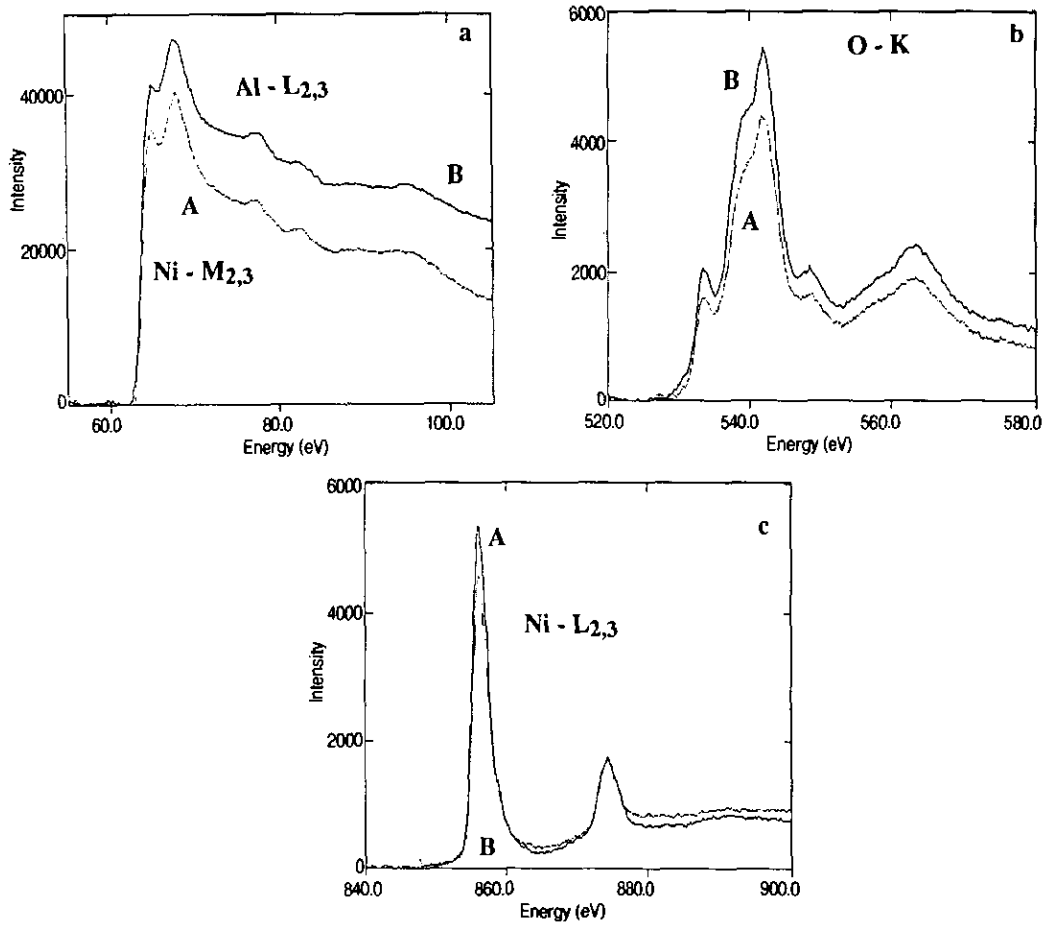

FIG. 4. Core loss spectra from the two regions A and B of Fig. 3. The Ni–M_{23} and Al–L_{23} edges are shown in (a), the O–K edge in (b) and the Ni–L_{23} edge in (c).

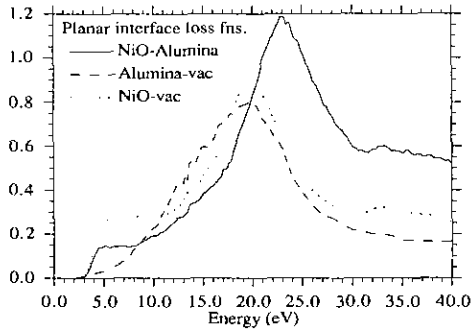

FIG. 5. Planar loss functions for the NiO–alumina interface and for the NiO and alumina free surfaces.

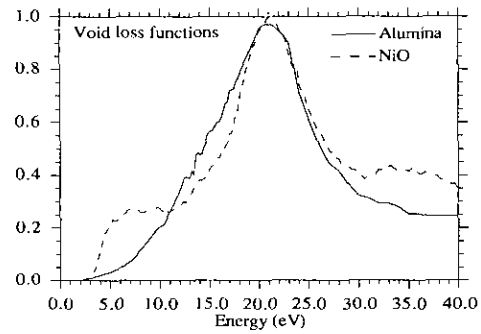

FIG. 6. Characteristic loss functions for a small void in NiO or alumina.

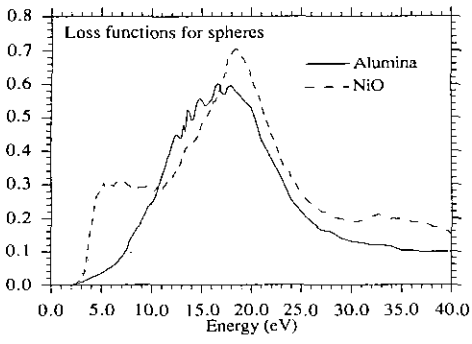

FIG. 7. Characteristic dipole loss functions for a small alumina or NiO spherical particle.

where the dielectric response of the two components are quite similar, spatial variations in the position of the loss peak are observed and may ultimately yield information about the void or pore fraction of the material.

Acknowledgments

We thank Drs. G. Wrobel, E. Payen and Mrs. C. Lamonier (University of Lille) for making available the mixed-oxide samples as well as Dr. Yuan Jun for supplying the dielectric data for NiO. Dr. Cadete Santos Aires and the project generally were supported by a grant from the EEC (Contract No. SCI 000314) for which we are grateful.

References

1. J. M. THOMAS, T. G. SPARROW, M. K. UPPAL, AND B. G. WILLIAMS, *Philos. Trans. R. Soc. A* **318,** 259 (1986).
2. A. J. F. METHERELL, *Adv. Opt. Elect. Microsc.* **4,** 263 (1971).
3. E. FERMI, *Phys. Rev.* **57,** 485 (1940).
4. R. H. RITCHIE, *Phys. Rev.* **106,** 874 (1957).
5. F. FUJIMOTO AND K. KOMAKI, *J. Phys. Soc. Jpn* **25,** 1679 (1968).
6. M. G. WALLS AND A. HOWIE, *Ultramicroscopy* **28,** 40 (1989).
7. U. UGARTE, Doctor of Science thesis, University of Paris-Sud (1990).
8. R. GARCIA MOLINA, A. GRAS-MARTI, A. HOWIE, AND R. H. RITCHIE, *J. Phys. C* **18,** 5335 (1985).
9. C. A. WALSH, *Philos. Mag. B* **59,** 227 (1989); *Philos. Mag. B* **63,** 1063 (1991).
10. T. L. FERRELL AND P. M. ECHENIQUE, *Phys. Rev. Lett.* **55,** 1526 (1985).
11. P. M. ECHENIQUE, A. HOWIE, AND D. J. WHEATLEY, *Philos. Mag. B* **56,** 335 (1987).
12. P. M. ECHENIQUE, J. BAUSELLS, AND A. RIVACOBA, *Phys. Rev. B* **35,** 1521 (1987).
13. P. BATSON, *Surf. Sci.* **156,** 720 (1985).
14. Z. L. WANG AND J. M. COWLEY, *Ultramicroscopy* **21,** 77, 335, and 347 (1987).
15. N. ZABALA AND A. RIVACOBA, *Ultramicroscopy* **35,** 145 (1991).
16. A. HOWIE AND C. A. WALSH, *Microsc. Microanal. and Microstructr.* **2,** 17 (1991).
17. D. W. MCCOMB AND A. HOWIE, *Ultramicrosc.*, **34,** 84 (1990).
18. A. HOWIE AND D. W. MCCOMB, "Proceedings EMSA Conference," p. 1150 (1992).
19. M. P. SOHIER, G. WROBEL, J. P. BONNELLE, AND J. P. MARCQ, *Appl. Catal. A* **84,** 169 (1992).
20. R. F. EGERTON, "Electron Energy Loss Spectroscopy," Plenum, New York (1986).
21. R. TEWS AND R. GRUNDLER, *Phys. Status Solidi B* **109,** 255 (1982).
22. R. D. LEAPMAN, L. A. GRUNES, AND P. L. FEJES, *Phys. Rev. B* **26,** 614 (1982).